CONF-861007--23

DE87 004956

CCD-BASED SYNCHROTRON X-RAY DETECTOR FOR PROTEIN CRYSTALLOGRAPHY--PERFORMANCE PROJECTED FROM AN EXPERIMENT

M. G. Strauss, I. Naday, I. S. Sherman

M. R. Kraimer and E. M. Westbrook

Argonne National Laboratory

Argonne, Illinois, 60439

DISCLAIMER

This report was prepared as an account of work sponsored by an agency of the United States Government. Neither the United States Government nor any agency thereof, nor any of their employees, makes any warranty, express or implied, or assumes any legal liability or responsibility for the accuracy, completeness, or usefulness of any information, apparatus, product, or process disclosed, or represents that its use would not infringe privately owned rights. Reference herein to any specific commercial product, process, or service by trade name, trademark, manufacturer, or otherwise does not necessarily constitute or imply its endorsement, recommendation, or favoring by the United States Government or any agency thereof. The views and opinions of authors expressed herein do not necessarily state or reflect those of the United States Government or any agency thereof.

Presented at the Nuclear Science Symposium, October 29-31, 1986, Washington, DC

To be published in the IEEE Trans. Nucl. Sci. NS-34, No. 1 (1987)

The submitted manuscript has been authored by a contractor of the U. S. Government under contract No. W-31-109-ENG-38. Accordingly, the U. S. Government retains a nonexclusive, royalty-free license to publish or reproduce the published form of this contribution, or allow others to do so, for U. S. Government purposes.

MASTER

DISTRIBUTION OF THIS DOCUMENT IS UNLIMITED

EBB

CCD-BASED SYNCHROTRON X-RAY DETECTOR FOR PROTEIN CRYSTALLOGRAPHY— PERFORMANCE PROJECTED FROM AN EXPERIMENT*

Michael G. Strauss, Istvan Naday, Irvin S. Sherman
Martin R. Kraimer and Edwin M. Westbrook

Argonne National Laboratory
Argonne, Illinois 60439

Abstract: The intense x radiation from a synchrotron source could, with a suitable detector, provide a complete set of diffraction images from a protein crystal before the crystal is damaged by radiation (2-3 min). An area detector consisting of a 40 mm dia. x-ray fluorescing phosphor, coupled with an image intensifier and lens to a CCD image sensor, was developed to determine the effectiveness of such a detector in protein crystallography. The detector was used in an experiment with a rotating anode x-ray generator. Diffraction patterns from a lysozyme crystal obtained with this detector are compared to those obtained with film. The two images appear to be virtually identical. The flux of 10^4 x-ray photons/s was observed on the detector at the rotating anode generator. At the 6-GeV synchrotron being designed at Argonne, the flux on an 80x80 mm^2 detector is expected to be $>10^9$ photons/s. The projected design of such a synchrotron detector shows that a diffraction-peak count $>10^6$ could be obtained in ~0.5 s. With an additional ~0.5 s readout time of a 512x512 pixel CCD, the data acquisition time per frame would be ~1 s so that ninety 1° diffraction images could be obtained, with approximately 1% precision, in less than 3 min.

I. Introduction

The advent of synchrotron x-ray sources over the past decade with their very high flux intensity, energy tunability, and small beam divergence, has created many new opportunities in the field of protein crystallography. Protein crystals are extremely labile when exposed to x rays, seldom lasting more than two days in the beam of conventional x-ray sources. Since protein crystals diffract weakly, one to two weeks of data collection may be required to record a complete 3-dimensional data set, so that data from many crystals must be merged. It should be possible to collect data much faster with synchrotron radiation so that an entire 3-dimensional data set could be obtained from just a single crystal, if a suitable detector were available.

The useful life of a typical protein crystal in an intense synchrotron x-ray beam is 2-3 min. We aim to record a complete data set on about 90 image frames each of 1° crystal rotation, within 3 min, which should yield a complete data set in all but the most demanding studies. This calls for data accumulation, readout, and storage of 90 frames in 2-3 min, which requires a data acquisition time of 1-2 seconds/frame.

The high x-ray intensities from synchrotron sources far exceed the count-rate capabilities of all counting-type detectors, such as gas proportional counters. On the other hand film, the most common integrating-type detector, can handle the high x-ray flux, but it is limited by its intrinsic chemical fog and its labor intensive nature[1]. Changing film on line is a slow, tedious process, while chemical film development and off-line microdensitometry are both time consuming and introduce nontrivial errors. To overcome the limitations of film, x-ray TV detectors have been developed over the past 20 years[2-5]. These TV detectors generally use the silicon intensified target (SIT) vidicon, a proven device but one with high readout noise level and therefore poor dynamic range. Solid-state area sensors, such as the charge-coupled device (CCD), have been recognized as possessing characteristics significantly superior to the SIT vidicon[6]. X-ray detectors using CCD sensors have been developed by Dalglish et al[7] and Eikenberry et al[8] but have not been applied to protein crystallography.

We report here the development of a CCD-based area x-ray detector for protein crystallography, with which we have now conducted basic feasibility experiments. We have evaluated this detector by recording diffraction patterns from hen egg-white lysozyme protein crystals, using x rays from a conventional rotating anode generator. From the results of this experiment we project that this detector should be capable of acquiring excellent diffraction data from protein crystals using advanced synchrotron sources, such as the one being designed at Argonne National Laboratory, at a rate of one frame per second with detection precision of 10^{-3}. To our knowledge this is the first time a CCD-based x-ray detector has been used in protein crystallography.

II. Basic Synchrotron X-Ray Detector System

A 2-dimensional integrating detector for synchrotron x rays is comprised of a combination of components, which include fluorescent phosphor, optics, image sensor, analog-to-digital converter, and data processors and stores. A diagram of the generic components and their function is shown in Fig. 1. X rays scattered from the protein crystal are absorbed in the phosphor thereby giving rise to fluorescent light. The light image is demagnified and focused on the image sensor (CCD) by the optical system which includes a lens system and/or a fiber optic taper and/or an image intensifier. Light photons impinging on the CCD create electrons which are collected in discrete pixels at the point of photon incidence. Thus, a 2-D image is formed in the CCD where the intensity of each point is determined by the number of electrons in the pixel. At the end of the accumulation period, the CCD is read out pixel by pixel thus producing video pulses. The pulses are digitized and temporarily stored in a fast buffer memory. When the CCD readout is completed, the next frame accumulation commences and the data previously stored in the buffer memory are transferred to the computer for permanent storage and display.

The specific design of a detector based on the scheme of Fig. 1 must be oriented towards the application of interest. The principal requirements for protein crystallography are listed in Table I. A detector area of at least 80x80 mm^2 is required in order to observe all the reflections from a typical protein crystal. Although the CCD might be used for direct detection of x rays, its area, where the

* Work performed under the auspices of the U.S. Department of Energy.

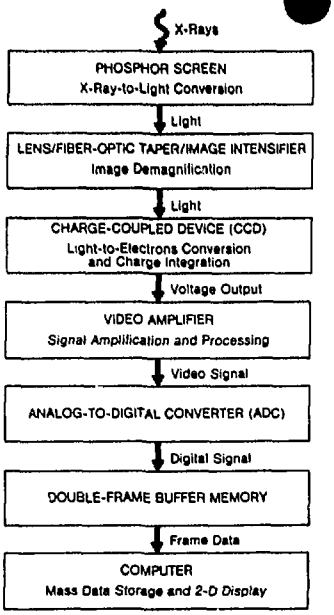

Fig. 1 Function flow chart of CCD-based synchrotron x-ray detector showing its generic components.

Table I

Detector Requirements for Protein Crystallography with Synchrotron X Rays

Photon energy (keV)	8-15
Detector flux (Xph/s/det. area)	10^9-10^{11}
Minimum detector area (mm^2)	80x80
Minimum spatial resolution (pixels)	512x512
Data acquisition* time (s/frame)	1-2
Diffraction-peak precision (%)	
Strongest peak	<1
1/100 Strongest peak	<10

* Data accumulation, readout & storage.

lateral dimension is 10-15 mm, is clearly inadequate. For this as well as other reasons we are using a large phosphor at the input and subsequently demagnifying the image to match the CCD size. The product of the fluorescent yield of the phosphor, the transmission efficiency of the optical system, and the quantum efficiency of the CCD is referred to as x ray-to-electron conversion efficiency. The conversion efficiency determines the average electron yield in the CCD pixel due to an incident x-ray photon on the phosphor. Since the full-well electron capacity of a pixel is limited, the conversion efficiency also determines the maximum pixel capacity in terms of x-ray photons. The system is designed for the highest conversion efficiency, consistent with the required signal-to-noise ratio. The maximum accumulation period per CCD frame is governed by the pixel saturation capacity. With detector input rates in excess of 10^9 x-ray photons/s, the exposure time per frame is expected to be less than 1 s while the computer/disk data transfer time may be longer. Without the fast buffer memory a full-frame CCD would be paralyzed during the data transfer period, thus reducing the framing rate.

III. Test Detector System

In order to project the design parameters for a detector to be used in protein crystallography with synchrotron x rays, a test detector was developed and evaluated in an experiment using a rotating anode x-ray generator as shown in Fig. 2. X rays scattered from the protein crystal form a diffraction pattern on the input phosphor which is then intensified with unity magnification. A 2-lens system demagnifies by 4 the intensified image and focuses it on the CCD cooled to -35°C. At the end of the exposure time the controller initiates a CCD readout and the video signals are digitized and stored on the computer disk. The image intensifier used here may not be required when the detector is used with synchrotron radiation. Since the x-ray intensity from the rotating anode generator is considerably lower than that from a synchrotron, much longer exposure times are required which, in turn, result in substantially higher CCD dark-current noise. The image intensifier is used here to assure reasonable signal-to-noise ratio for weak signals. The principal specifications of the components of this detector are given in the Appendix.

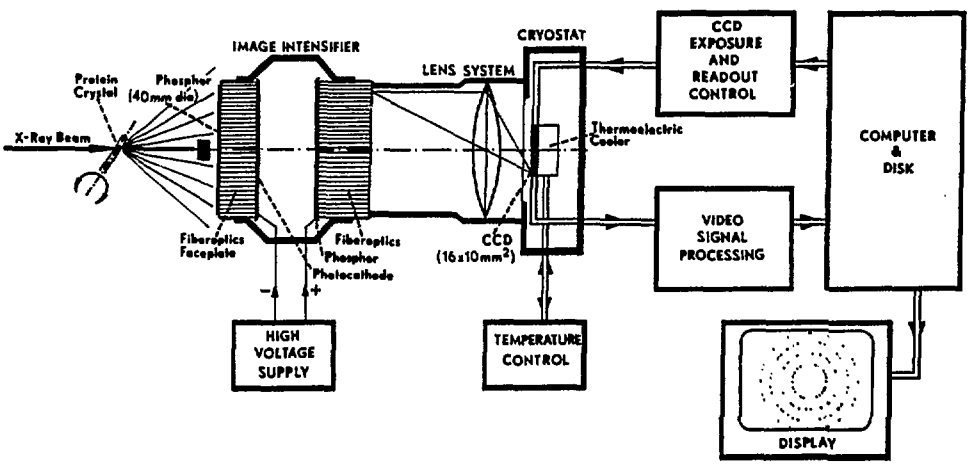

Fig. 2 Basic components of CCD-based detector system as used with a rotating anode x-ray generator in a protein crystallography experiment.

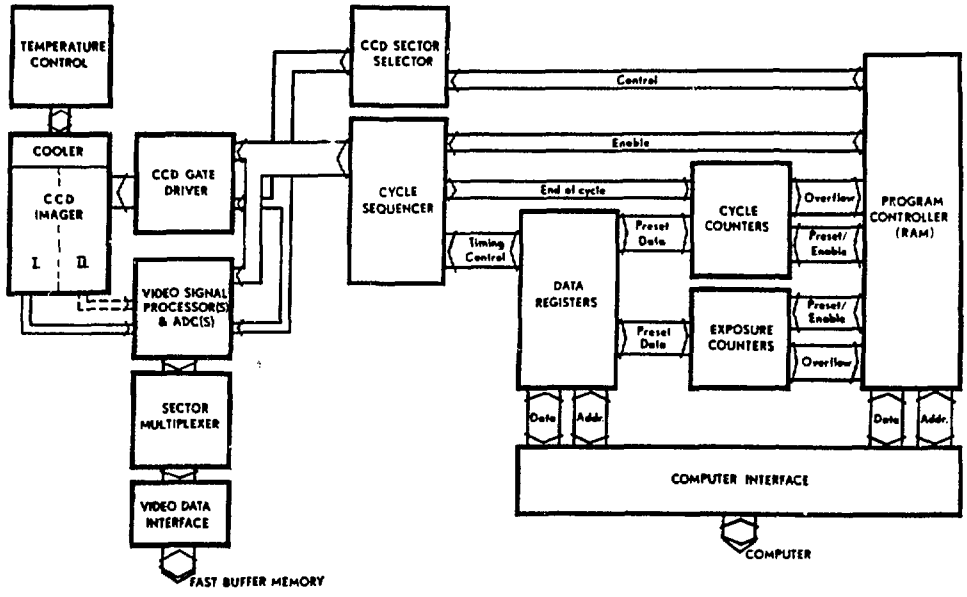

Fig. 3 Scheme of CCD controller showing how CCD operations and video signal processing are executed. CCDs of different type and size are accomodated by entering the appropriate program into the random access memory (RAM) and the desired parameters into the data registers.

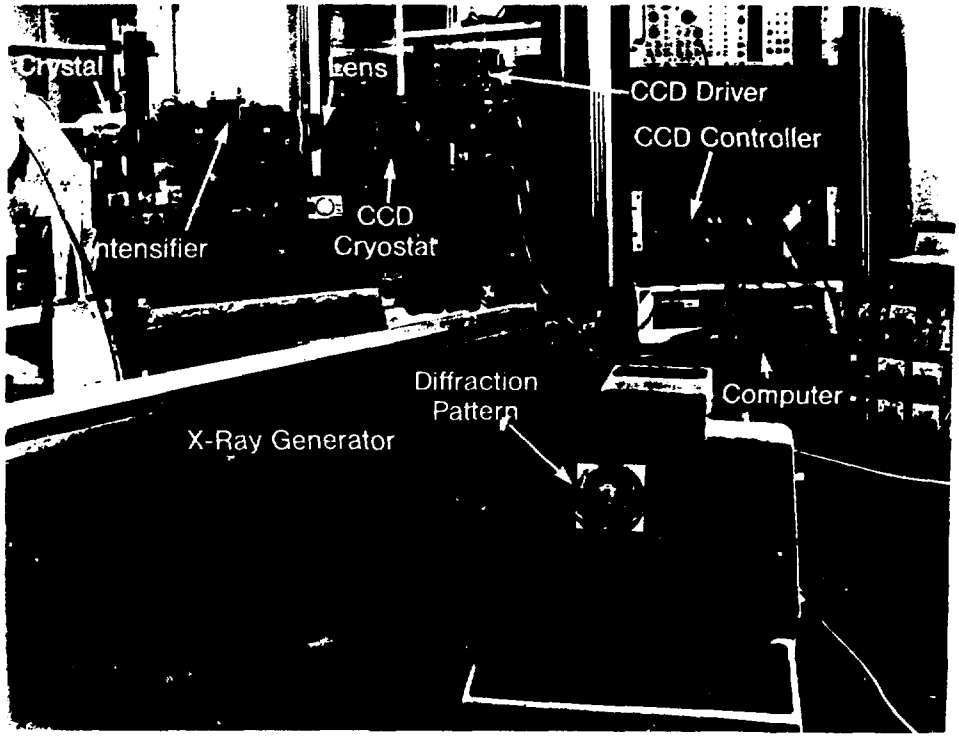

Fig. 4 Photograph showing the CCD test detector system mounted at our Elliot GX20 rotating anode x-ray generator during a protein crystallography experiment as illustrated in Fig. 2.

The operations of the CCD and the processing of the video signals are executed by the CCD controller. A detailed block diagram of the controller is shown in Fig. 3. The controller was developed for several different CCD-based detectors. In the present discussion only the features pertaining to protein crystallography are described. The controller can operate CCDs having virtually any pixel matrix size and having configurations such as full frame, frame transfer, and multiple sector[9]. CCDs with separate readout registers for each sector can be read out in parallel with separate ADCs. The video data are then multiplexed into the buffer memory.

The sector selector routes the gate signals to the vertical and horizontal CCD registers of the selected sector(s) and enables the corresponding ADC(s). The CCD readout rate, video signal processing mode (normal or double-correlated sampling), number of pixels in the frame, exposure time, etc., are entered into the data registers from the computer. Each of the above CCD configurations requires a different sequence of operations, such as exposure for a preset time, shift data from image area to storage area, read out with or without binning, etc. The program controller, which consists of a random access memory (RAM), controls the sequence of these operations. The program appropriate for a given CCD type and size is entered into the RAM from the computer.

A photograph of the experimental setup described in Fig. 2 is shown in Fig. 4. The detector system is mounted at our Elliot GX20 rotating anode generator using a CuKα emission line. The generator was operating with a 200 μm focus, 40 kV, and 40 mA beam current. The x-ray beam was monochromated with graphite. The phosphor was 45 mm from the crystal. The crystal was mounted on the ϕ spindle of an Enraf Nonius rotation camera. With the detector lens removed, the CCD can be seen through the cryostat glass window (Fig. 5).

IV. Test Detector Performance

A diffraction pattern was obtained with the CCD test detector as shown in Figs. 2 and 4. The crystal sample of tetragonal hen egg-white lysozyme was 0.5 x 0.5 x 0.1 mm^3 rotating through an angle of 2^o during the course of the exposure. The x-ray beam was defined by an adjustable collimator to match the crystal size (~0.5x0.5 mm^2). The diffraction pattern obtained in 14 min is shown in Fig. 6. For comparison a 60 min exposure on film (Kodak DEF-5) is shown in Fig. 7. Both, the detector and film were 45 mm from the crystal. Since the detector was only 40 mm in diameter, it could not capture the outer part of the diffraction pattern. The size and positions of the

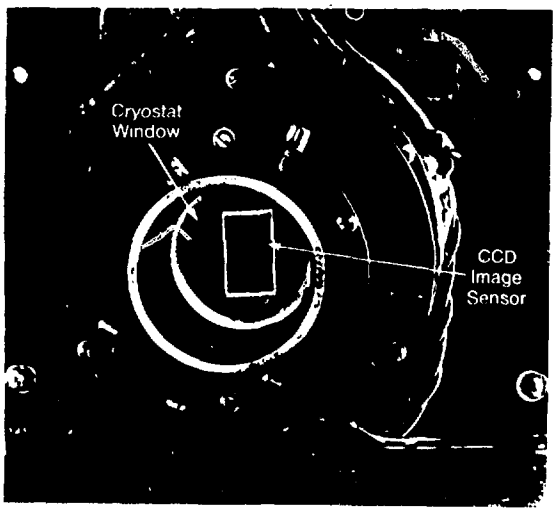

Fig. 5 Photograph of the CCD seen through the cryostat glass window when the lens (Fig. 4) was removed.

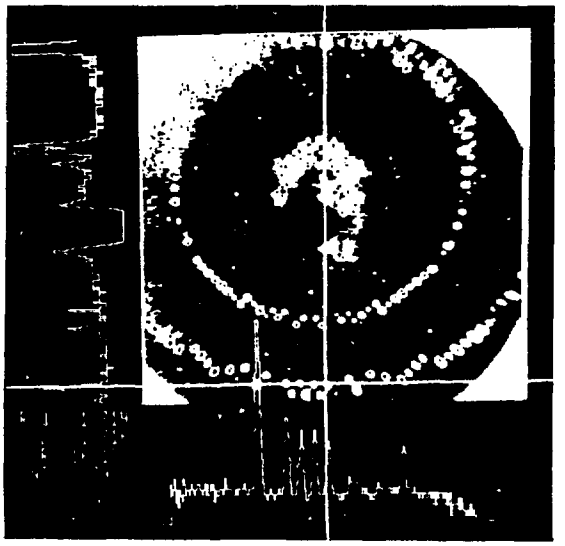

Fig. 6 Diffraction pattern, obtained with the CCD test detector in 14 min., of a tetragonal hen egg-white lysozyme crystal rotating through 2^o during the exposure. Note the horizontal and vertical peak profiles which permit evaluation of the diffraction spots at a glance.

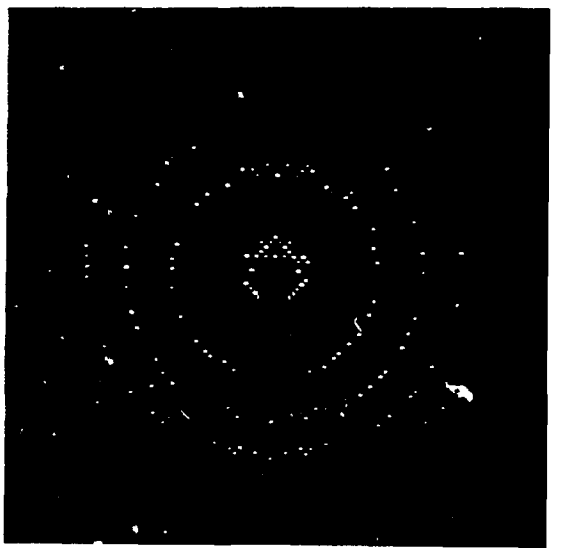

Fig. 7 Diffraction pattern, obtained on Kodak DEF-5 film in 60 min, of the same lysozyme crystal used with the CCD test detector in Fig. 5. Note that this image is virtually identical to that in Fig. 5 except that the CCD detector was smaller than the film and therefore, it could not capture the outer part of the diffraction pattern.

beam stops in the two photographs were also slightly different. An examination of the two photographs shows the two images to be virtually identical. The lens system showed considerable vignetting which is exhibited as off-center attenuation. In addition, CCDs have some pixel-to-pixel variation in sensitivity. To correct for these nonuniformities, an image of a uniform x-ray flood was obtained and normalizing factors relative to the average pixel contents were calculated for each pixel. Figure 6 is a normalized image obtained by multiplying the pixel signals in the raw image by these factors.

The cosmetic quality of this first detector picture is similar to that of a proof print. It was obtained by photographing the monitor screen (Fig. 4) which had only 16 gray levels. The data, digitized with a 12-bit ADC, showed a peak-intensity range of over 100:1 which cannot be adequately displayed with only 16 gray levels. Many spots on the monitor are therefore excessively broad and show overflow on the display. Even on film, which displays continuous variation in intensity, relative peak intensities are not easily perceived. A video display with cursors (Fig. 6) can instantly project peak profiles with which spots can be evaluated at a glance with respect to intensity and spatial resolution.

The legend on Fig. 6 indicates that the field of view in the CCD extends from pixel row 1-314 and pixel column 1-316, that the horizontal cursor is on row 16 and the vertical cursor on column 152, and that the intensity at the cursors' intersection, given by the digital number (DN) of the ADC, is 79.

The operation of the test detector with our rotating anode x-ray generator was evaluated in terms of several performance criteria and the results are listed in Table II. The x-ray flux on the detector was obtained from the integral of the full image in Fig. 6, which includes the diffraction peaks and the diffuse background. The intensity of the incident beam was measured with a calibrated phosphor-photomultiplier detector. From these measurements the scattering efficiency of our lysozyme crystal in this experiment geometry was found to be about 10^{-3}.

The maximum counts in a peak correspond to the peak saturation-capacity. When one or more pixels in a peak reach the full well level the peak is said to have maximum x-ray count capacity or saturation capacity. The correspondence between x-ray counts in the peak and electrons in the CCD pixel well is determined by the conversion efficiency, which is the CCD electron yield per x-ray photon on the input phosphor. This value was obtained from the integral of a peak due to a measured input x ray beam intensity. It is in agreement with the value obtained by considering the contributions of all individual system components. The exposure time, or accumulation time per frame, is determined by dividing the peak saturation-capacity by the intensity of the strongest peak. If the peak is situated on a background, the exposure time must be reduced accordingly to avoid pixel overflow.

The intrinsic FWHM spatial resolution of the detector was determined from a step response measurement observed when an extended x-ray beam was partially covered by lead foil. The step response measured from 10%-90% was less than 2 pixels, corresponding to the FWHM line response at the input phosphor of 200 μm. The FWHM of a diffraction peak measured ~500 μm at the phosphor screen, approximately the size of our lysozyme crystal.

The dynamic range, defined as the ratio of the integral of the strongest peak to the rms fluctuations over the same area (81 pixels) was 2×10^2, lower than expected due to the unusually high background of the image intensifier in the test detector.

The dark current background of the CCD at -35°C and with 860 s exposure, was approximately 4% of the saturation level, corresponding to ~120 e^- rms dark current noise per pixel. The CCD read noise and the digitization noise were 60 e^-/pixel and 42 e^-/pixel, respectively. The total electronic noise due to the CCD dark current, CCD readout and the ADC digitization (image intensifier excluded) was calculated to be 2×10^{-4} of a saturation peak. The uncertainty due to these fluctuations is considerably less than that due to the x-ray statistics in the peak $(6\times10^4)^{-1/2}$.

Table II

Performance of X-Ray Detectors

	Test Detector (Experiment values)	Synchrotron Detector (Projected values)
X-ray Source	Rotating anode gen. (40kV, 40mA)	6-Gev synchrotron (bending magnet)
Photon energy (keV)	8	8-15
Beam intensity on crystal (Xph/s)	2×10^7	2×10^{12}
Lysozyme crystal size (mm^2)	0.5x0.5	0.5x0.5
Detector area (mm^2)	40x40	80x80
Frame size (pixels)	314x316	512x512
Detector flux (Xph/s/det. area)	10^4	4×10^9
Intensity of strongest diffraction peak (Xph/s)	60	6×10^6
Conversion efficiency (e^-/Xph)	90	1
Pixel saturation level (Xph)	5×10^3	7×10^5
Diffraction peak saturation capacity (Xph)	6×10^4	3×10^6
Detector FWHM resolution (μm)	200	160
Diffraction peak FWHM (μm)	500	500
Dynamic range: saturation peak/rms elect. noise	2×10^2	5×10^3
Accumulation time (s/frame)	860	0.55
CCD readout time (s/frame)	1	0.5
Data storage time (s/frame)	5	1-2

V. Projected Synchrotron X-Ray Detector

The evaluation of the test detector provides the necessary data to project the performance of a detector for protein crystallography with synchrotron x rays. From Figs. 6 and 7 it is apparent that a detector with a lateral dimension of 80 mm will be more adequate than one with only 40 mm. Using a 512x512 pixel CCD (14x14 mm^2) with an 80 mm detector would give nearly the same spatial resolution as that obtained with the 40 mm test detector and 314x316 pixels (9.5x9.5 mm^2). A demagnification of ~6 would be required for the 80 mm detector as compared to 4 which was used in the test detector.

The increase in flux from the synchrotron source as compared with that from a rotating anode generator is the paramount factor to be considered. The expected flux[10] on a 0.5x0.5 mm^2 crystal from a bending magnet of the 6-GeV synchrotron being designed at Argonne is $2x10^{12}$ x-ray photons/s (Table II). This corresponds to 10^5 increase in x-ray intensity and would subject the detector to a flux of $4x10^9$ x-ray photons/s.

In order to obtain the maximum x-ray count in a short exposure time, the conversion efficiency should be near unity[11,12]. If it is less than unity only a fraction of the incident x-ray photons are recorded and a longer exposure time would be required to obtain peak saturation-capacity. If it is greater than unity, the saturation capacity in terms of x rays is smaller and would, therefore, result in a reduced statistical precision. When the conversion efficiency is near unity, the statistical uncertainty in the peak is on the order of two times the x-ray statistics, provided the electronic noise is much smaller than these statistics. We believe that an adequately low noise can be realized and therefore a conversion efficiency of unity can be used.

The ultimate limit of precision in this protein crystallography detector is determined by the x-ray statistics and, in turn, by the peak saturation-capacity. Scaling the value obtained with our test detector (Table II) by the lower conversion efficiency and higher demagnification (fewer pixels/peak) we obtain a peak saturation-capacity of over $3x10^6$ x-ray photons. This would give a very adequate statistical precision even for small peaks that are 1% of maximum. For a lysozyme crystal the most intense peak will reach saturation capacity in 550 ms.

The intrinsic spatial resolution of the detector is essentially limited by the number of CCD pixels. For a crystal larger than this intrinsic resolution (80 mm/512), the diffraction peak FWHM will be governed primarily by the crystal size.

The sources of electronic noise in the detector are CCD dark current, CCD readout, and ADC digitization. In synchrotron applications where the readout is fast, read noise is the dominant source. Increasing readout rate results in higher signal-sampling fluctuations and hence larger uncertainties. With an accumulation time of ~0.5 s/frame and conventional data storage time limitation >1 s/0.5 MB frame, the CCD readout speed need not be faster than 0.5 s/frame in order to meet our data acquisition objective of 1 frame/s. At this readout rate (0.5 Mpixel/s) the read noise is ~100 e^- rms/pixel and the total electronic noise is $2x10^{-4}$ of the saturation peak (inverse dynamic range), which is only 1/3 of the x-ray statistics. Thus, the uncertainty in a saturation peak, using a conversion gain of unity, is not expected to be greater than twice the uncertainty in the x-ray statistics.

VI. Discussion

Our diffraction experiment with a lysozyme crystal, using a rotating anode x-ray generator, has shown that a detector based on the scheme of Fig. 1 can meet the requirements for protein crystallography with synchrotron x rays as outlined in Table I. In practice the requirements may be broader than indicated. Tetragonal lysozyme crystals scatter strongly, whereas crystals to be studied with this detector may, in general, scatter more weakly, may be smaller, may have more diffraction peaks, or may be more sensitive to radiation damage than lysozyme. The basic detector configuration of Fig. 1 has considerable flexibility in the design to accommodate a wide range of requirements.

Since during readout the detector is dead, fast readout is desirable, especially when exposure times are long and the useful life of the crystal is short. The CCD controller has a readout-rate capability of 5 Mpixels/s or 50 ms per 512^2 pixel frame when used with a 5 MHz ADC and a 10 MB/s VME buffer memory. The noise at this readout rate would increase accordingly to $2x10^{-3}$ of the saturation peak. The increase in noise could, however, be avoided or ameliorated by using a frame-transfer CCD or larger CCD where for the same pixel size the signal-to-noise ratio increases in proportion to $(X \cdot Y)^{1/2}$ where X and Y are the number of pixels in the CCD row and column, respectively. If the CCD had several sectors which could be read out in parallel, faster readout could be accomplished without, or with reduced, additional noise. A larger CCD would also provide better spatial resolution, which, judging from Fig. 6, would be desirable.

When the detector is used at a fast framing rate it is imperative that the afterglow from the phosphor is sufficiently low that the diffraction pattern of one frame does not persist during the exposure of the next frame. The Gd_2O_2S phosphor used in the test detector has not been evaluated with respect to afterglow nor with respect to linearity. The characteristics of the phosphor also affect the design of the optical system. With a phosphor yielding 200 light photons per x-ray photon and fiber optic coupling between an 80x80 mm^2 phosphor and a 512^2 pixel CCD one can expect a conversion efficiency of unity. If, however, the phosphor yield is significantly lower, additional optical gain may be required unless a larger CCD is used permitting less demagnification where more of the phosphor light is transmitted through the fiber-optic taper to the CCD. Using a larger CCD is preferable to using an image intensifier as an image intensifier could introduce afterglow problems, would degrade the spatial resolution, and would increase the statistical uncertainty and noise. The combination of image intensifier and lens optics, used in the test detector, was selected for expedience rather than as the choice system for a synchrotron detector.

The treatment of this work clearly deserves more detailed coverage than was given here. However, time constraints and space did not permit going into greater depth.

VII. Conclusion

A CCD-based x-ray detector has been used successfully for imaging diffraction patterns from a protein crystal using a rotating anode x-ray generator. Based on this detector performance, we project that with a 10^5 increase in flux, expected from a synchrotron source, one can obtain a complete 3-dimensional set of reflections in 2-3 min, before radiation damage destroys a typical protein crystal.

Several design changes are being considered for future synchrotron x-ray detectors. A CCD larger than 512x512 pixels would be desirable if the longer readout time can be tolerated. It would be better yet, if a larger frame-transfer device was available or if the CCD had several sectors which could be read out in parallel. We will explore the use of a fiber-optic taper for coupling the phosphor to the CCD either instead of, or perhaps initially in combination with, an image intensifier and lens system. Phosphors will be characterized with respect to afterglow (persistence) and fluorescent yield so that they can be appropriately selected to meet specific detector requirements such as fast framing rate.

The x-ray detector described here is based on opto-electronic semiconductor technology. This is a rapidly developing field which undoubtedly will continue to advance the state-of-the-art of detectors for protein crystallography.

Acknowledgments

The assistance of R. L. Stanfield in conducting the crystallography experiments, and the consultations with R. T. Daly regarding the fast buffer memory are gratefully acknowledged.

References

[1] J. R. Helliwell, "The Use of Electronic Area Detectors for Synchrotron X-Radiation Protein Crystallography with Particular Reference to the Daresbury SRS," Nucl. Instr. and Meth, 201, 153-174 (1982).

[2] U. W. Arndt and B. K. Ambrose, "An Image Intensifier--Television System for the Direct Recording of X-Ray Diffraction Patterns," IEEE Trans. Nucl. Sci, NS-15(3), 92-94 (1968).

[3] G. T. Reynolds, "Image Intensification Techniques Applied to the Study of X-Ray Diffraction Patterns," IEEE Trans. Nucl. Sci. NS-17(3), 310-317 (1970).

[4] U. W. Arndt, "X-Ray Television Area Detectors," Nucl. Instr. and Meth. 201, 13-20 (1982).

[5] J. R. Milch, S. M. Gruner and G. T. Reynolds, "Area Detectors Capable of Recording X-Ray Diffraction Patterns at High Count-Rates," Nucl. Instr. and Meth. 201, 43-52 (1982).

[6] S. M. Gruner, J. R. Milch and G. T. Reynolds, "Survey of Two-Dimensional Electro-Optical X-Ray Detectors," Nucl. Instr. and Meth. 195, 287-297 (1982).

[7] R. A. Dalglish, V. J. James, and G. Tubbenhauer, "A Two-Dimensional X-Ray Diffraction Pattern Sensor Using a Solid State Area Sensitive Detector," Nucl. Instr. and Meth. 227, 521-525 (1984).

[8] E. F. Eikenberry, S. M. Gruner and J. L. Lowrance, "A Two-Dimensional X-Ray Detector with a Slow-Scan Charge-Coupled Device Readout, " IEEE Trans. Nucl. Sci., 3(1), 542-545 (1986).

[9] R. D. McGrath, D. E. Russel, J. Frank and S. Popik, "A Very Large Format Multimode Imager," in Proc. of Electronic Imaging 85 Conf., Boston, MA, Oct. 7-10, 1985, pp 156-159.

[10] "6-GeV Synchrotron X-Ray Source," Supplement B. Argonne National Laboratory Report LS-51, pp 71-73 (March 1986).

[11] M. G. Strauss, I. Naday, I. S. Sherman and N. J. Zaluzec, "CCD-Based Parallel Detection System for Electron Energy-Loss Spectrometry and Imaging," In Proc. of Conf. on Frontiers of Electron Microscopy in Material Science, Argonne National Laboratory, Argonne, IL, April 20-23, 1986. Ultramicroscopy (in press).

[12] H. W. Deckman and S. M. Gruner, "Format Alterations in CCD Based Electro-Optic X-Ray Detectors," Nucl. Instr. and Meth, A246, 527-533 (1986).

Appendix

Principal Specifications of Test Detector Components

Input Phosphor
- Type: P-43, Gd_2O_2S:Tb (Trimax 2)
- Peak Emission: 545 nm (Green)
- Layer Thickness: 80 μm
- Diameter: 40 mm
- Manufacturer: 3M Corp., St. Paul, MN

Image Intensifier
- Type: 2 Stage (Model No. 1268)
- Focusing Method: Electrostatic (Generation I)
- Magnification: 1
- Photocathode: Spectral Response: S-20 Extended Red
  - Quantum Efficiency: 11%
  - Diameter: 39 mm
- Phosphor: P-20, $ZnCdS_2$:Ag
- Resolution at 3% MTF: 40 lp/mm
- Manufacturer: Varo, Inc., Garland, TX

Lens System
- Two Nikkor lenses coupled "nose-to-nose"
- Overall magnification: 0.25
- Objective lens:
  - Focal length: 200 mm
  - F-number: 4
- Image lens
  - Focal length: 50 mm
  - F-number: 1.2
- Manufacturer: Nippon Kogaku K. K., Tokyo, Japan

CCD Imager
- Type: SID 501 EX
- Number of pixels: 512x320
- Pixel size: 30x30 μm^2
- CCD size: 9.6x15.36 mm^2
- Full well capacity: $5x10^5$ electrons
- Architecture: Frame transfer (used in "full array" mode)
  - Thinned, back illuminated
  - 3-phase
- Manufacturer: RCA, Lancaster, PA